

# Angular correlations in the cosmic gamma-ray background from dark matter annihilation around intermediate-mass black holes

Marco Taoso,<sup>1,2</sup> Shin'ichiro Ando,<sup>3</sup> Gianfranco Bertone,<sup>2</sup> and Stefano Profumo<sup>4</sup>

<sup>1</sup>*INFN, Sezione di Padova, via Marzolo 8, Padova, 35131, Italy*

<sup>2</sup>*Institut d'Astrophysique de Paris, UMR 7095-CNRS,*

*Université Pierre et Marie Curie, 98bis boulevard Arago, 75014 Paris, France*

<sup>3</sup>*California Institute of Technology, Mail Code 130-33, Pasadena, California 91125, USA*

<sup>4</sup>*Santa Cruz Institute for Particle Physics and Department of Physics,  
University of California, Santa Cruz, California 95064, USA*

Dark matter (DM) annihilation could in principle contribute to the diffuse cosmic gamma-ray background (CGB). While with standard assumptions for cosmological and particle physics parameters this contribution is expected to be rather small, a number of processes could boost it, including a larger-than-expected DM annihilation cross-section, or the occurrence of DM substructures such as DM mini-spikes around intermediate-mass black holes. We show that angular correlations of the CGB provide a tool to disentangle the signal induced by DM annihilation in mini-spikes from a conventional astrophysical component. Treating blazars as a known background, we study the prospects for detecting DM annihilations with the Fermi Gamma-Ray Space Telescope for different choices of DM mass and annihilation channels.

## I. INTRODUCTION

The identification of nonbaryonic dark matter (DM) is still an open problem. Weakly interacting massive particles (WIMPs) are among the best motivated DM candidates, due to their connections with several, independently formulated particle physics theories beyond the Standard Model, and also in view of their intriguing phenomenology (see Refs. [1, 2, 3, 4] for reviews). WIMPs are actively searched for with underground detectors, with searches for related signatures with the Large Hadron Collider, and, indirectly, through the detection of their annihilation products.

In particular, within the latter detection technique, anti-matter and gamma-ray signals from WIMPs annihilation are actively being searched for with the PAMELA (Payload for Anti-Matter Exploration and Light-nuclei Astrophysics) satellite and with the Fermi Gamma-ray Space Telescope (formerly known as GLAST), both currently taking data. PAMELA has actually already found an interesting feature in the positron ratio spectrum Ref. [5], made even more interesting by the recent ATIC data [6]. This feature could be explained in terms of the annihilation or decay of DM particles, although the gamma-ray flux implied by these models severely constrain this interpretation (see Ref. [7] and references therein). Several other indirect (often conflicting) hints pointing towards the existence of particle DM have been proposed over the last few years, and it is therefore important to search for strategies that allow to robustly and conclusively disentangle a DM signal from a more mundane standard astrophysical origin.

The origin of the cosmic gamma-ray background (CGB) measured with EGRET [8] is currently uncertain and the most favored explanation calls for the existence of an unresolved population of active galactic nuclei (AGNs). Recent determinations of the gamma-ray luminosity functions (GLF) show however that unresolved

blazars alone can explain only 20-50% of the measured CGB [9], therefore leaving room for other gamma-ray emitters. Besides other standard astrophysical sources, e.g. unresolved gamma-ray emission from clusters of galaxies [10, 11] or normal galaxies [12], cosmological WIMPs annihilation could also contribute to the CGB [13, 14, 15, 16].

Assuming a smooth profile for DM halos, the absence of intense gamma-ray emission from the center of our galaxy constrain the DM contribution from cosmological halos to be rather low [17], but it has been shown that the presence of substructures can largely boost this signal without being in conflict with galactic bounds [18, 19]. Here we focus on *mini-spikes*, i.e. large DM overdensities that might form around intermediate-mass black holes (IMBHs), due to the adiabatic contraction of the DM density profile during the IMBHs' formation and growth [20]. Unlike the case of a DM spike around the central supermassive black hole (SMBH) of our galaxy, which would inevitably be disrupted by the combination of several astrophysical processes [13, 21, 22], the depletion of mini-spikes is expected to be far less efficient. It has been shown that taking into account the contribution from cosmological mini-spikes, DM annihilations can largely contribute to the measured CGB [18], while spikes around SMBHs can provide only moderate boosts [23].

In addition, mini-spikes in the Milky Way or nearby galaxies such as M31 could be detected with neutrino telescopes [24], boost anti-matter fluxes [25] or individually resolved by gamma-ray telescopes such as the Fermi LAT [20, 26, 27]. The simultaneous detection of several sources with the same energy spectra, showing a cut-off at the DM mass, would be a smoking gun for WIMPs annihilation. On the contrary, it is difficult to extract straightforward evidences for DM annihilation from the study of the CGB spectrum itself. A search for these objects based on a HESS survey of the Galactic plane region has already allowed to set some interesting con-

straints on the mini-spikes scenario [28]. However, additional information can be extracted by the anisotropy data [29, 30, 31, 32, 33, 34]. In particular, the CGB angular power spectrum from blazar and from DM annihilation in halos or subhalos are quite different, due to their different energy spectra, cosmological distribution, and radial emissivity profiles. Therefore, the study of the CGB angular power spectrum provides, in principle, a robust and direct tool to discriminate between the two different scenarios. Assuming the unresolved blazar contribution as a “known” background, DM annihilation could be detected with roughly 2 years of Fermi data, provided they contribute a fraction  $\gtrsim 0.3$  of the CGB at 10 GeV [30].

In this paper we perform the angular anisotropy analysis for the case of cosmological DM mini-spikes around black holes. We compute the angular power spectrum for different DM benchmark setups, varying the particle mass and the annihilation channel, and for different gamma-ray energies, showing that the results are quite sensitive to all of these variables. We also discuss the possibility to distinguish with Fermi data the mini-spike scenario from the case of substructure-dominated emission.

The remainder of the paper is organized as follows: Section II is devoted to a discussion of IMBH formation and to a summary of the results of recent numerical simulations. In Sec. III, we compute the contribution to the CGB mean intensity from DM annihilation in cosmological mini-spikes and from blazars, while in Sec. IV we compute the angular power spectrum for the two cases. A mixed scenario is presented in Sec. V, where we also discuss prospects for detecting DM annihilation with the Fermi Telescope and the effect of changing particle DM parameters and the gamma-ray energy at which the anisotropy is studied. Finally, conclusions are presented in Sec. VI. Throughout this paper, we adopt a flat  $\Lambda$ CDM model with the cosmological parameters from WMAP 5-year data [35].

## II. INTERMEDIATE MASS BLACK HOLES

### A. IMBH formation

Black holes in the range  $20 \lesssim M_{bh}/M_\odot \lesssim 10^6$ , are commonly dubbed as IMBHs (see Ref. [36] for a review). Despite the lack of conclusive observational evidence for the existence of IMBH, many clues have been accumulated during the last few years, among which the most significant is perhaps the detection of ultra luminous X-ray sources (ULXs), interpreted in terms of accreting IMBHs [37, 38]. Although alternative explanations have also been proposed [39, 40], they seem to be problematic or in some cases ruled out [36, 41], suggesting that at least a fraction of the observed ULX sources are indeed IMBHs. Furthermore, the presence of SMBHs at high redshifts, as indicated by the detection of high red-

shift quasars at  $z \sim 6$  in the Sloan Digital Sky Survey [42, 43, 44], favors a formation scenario with rapid accretion and mergers from massive seed BHs [45]. Theoretically, this hierarchical scheme would also help explain the tight observed correlations between the SMBH mass and the host galaxy properties. IMBHs themselves could be the remnants of first stars, also referred to as Pop III stars [36]. These stars, the first formed in the Universe, are generally predicted to be very massive, as a consequence of their extremely low metallicity and the absence of wind and pulsations. While the fate of Pop III stars with masses in the range  $100 \lesssim M/M_\odot \lesssim 250$  is perhaps to explode due to pair instability, and to leave no compact remnant, heavier stars finally collapse directly to IMBHs, with little mass loss. Reference [20] investigated this formation scenario, by following the evolutions of the BHs host halos and taking into account IMBH mergers, and concluded that at  $z = 0$  a Milky-Way-sized halo should host a population of roughly 1000 unmerged IMBHs, with masses in the range  $10^2 - 10^3 M_\odot$ .

Here we consider an alternative IMBH formation scenario, proposed in Ref. [46] and further investigated in Refs. [20, 47]. In this framework, IMBHs are formed from gas collapsing in DM mini-halos at high redshifts. In massive enough halos, the molecular hydrogen cooling is very efficient and a proto-galactic disk is formed at the center. Gravitational instabilities in the disk then trigger an effective viscosity that drives an inflow of the gas lying in the low tail of the angular momentum distribution. In the absence of halo mergers, the process continues until the explosion of the first generation of supernovae, which heats up the disk. The mass transferred to the center of the halo undergoes gravitational collapse and a BH is then rapidly formed. The condition that the BHs formation timescale be shorter than the major merger timescale and that enough molecular hydrogen be present to form a pressure support disk, sets a lower limit on the mass of the host halo, i.e.,  $M_{cr} = 10^8 M_\odot$  at the reionization redshift  $z_{re}$ . The IMBH mass function is predicted to be a log-normal, with a peak at  $M_{BH} = 2.1 \times 10^5 M_\odot$  and a spread  $\sigma_{BH} = 0.9$ .

Reference [20] studied the population of IMBHs that would result from the aforementioned formation scenario in our own Galaxy. Specifically, the authors simulated the formation of a Milky-Way-like DM halo starting from mini-halos at high redshifts, following the hierarchical merger history of the latter until  $z = 0$  in the context of a  $\Lambda$ CDM model for structure formation. In that analysis, the formation of IMBHs in a given halo follows the prescription given in Ref. [46], and pair BH mergers occur if the pair distance is lower than 1 kpc.

IMBH formation is absent after reionization,  $z < z_{re}$ , since most of the molecular hydrogen, the main baryonic coolant, is ionized. In the simulation of Ref. [47], the authors find that IMBHs formation is highly suppressed for  $z > z_{re}$  since the suitable hosts for BH formation become increasingly rare as redshift increases. Therefore, according to Ref. [47], the formation redshift distribution

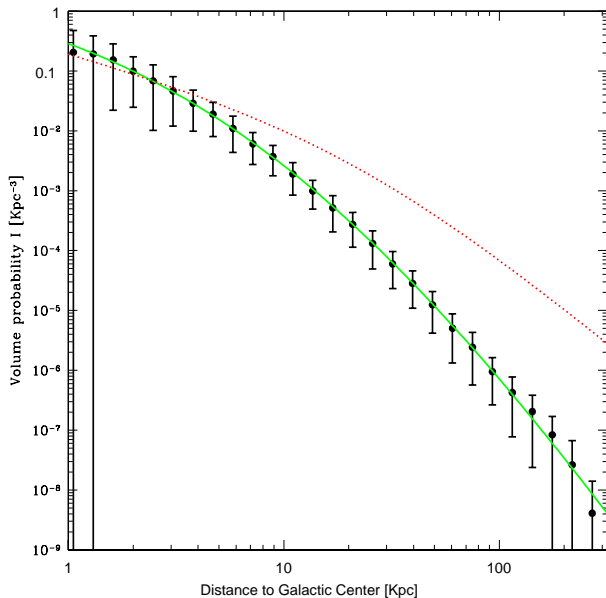


Figure 1: Radial distribution of the IMBH population in the Milky Way from the numerical results of Ref. [20]. The points refer to an average among the 200 Monte Carlo realizations of the Milky Way halo and error bars show the scatter among realizations. The solid line is an analytical fit and the dotted line is a NFW profile.

is peaked at  $z_{re}$ .

The authors performed 200 statistical realizations of the IMBH population providing for each IMBH its distance from the center of the galaxy, its mass and the surrounding DM distributions. The average number of unmerged IMBHs is  $N_{BH} = 101 \pm 22$ . The radial distribution of the IMBH population is described by the volume probability,  $g(r)$ , shown in Fig. 1 for an average realization among the 200 realizations of the IMBH population in the Milky Way. The function  $g(r)$  is simply defined as the probability to find an IMBH at a radial distance  $r$  from the Galactic center, in a spherical shell of thickness  $dr$ . The volume probability function is normalized to 1 between 1 kpc and the maximal distance from the Galactic center at which an IMBH is found, i.e. roughly 300 kpc. The error bars in the plot reflect the scatter among the 200 realizations.

The distribution is well fitted by the analytical function

$$g(r) = 5.9610^{-2} \left[ 1 + \left( \frac{r}{9.1 \text{ kpc}} \right)^{0.51} \right]^{-10.8} \text{ kpc}^{-3}.$$

The logarithmic slope,  $\gamma = d \log g / d \log r$ , is 1.5 at 1 kpc and 4.5 at 200 kpc, and therefore the resulting distribution is cuspier than a Navarro-Frenk-White profile (NFW) [48], shown in Fig. 1 for comparison.

Starting from the simulation of the IMBH population in the Milky Way halo in Ref. [20], the catalog can be adapted for other galaxies by rescaling the total number

of objects by the ratio between the host halo masses, and the galactocentric distance by the ratio of virial radii,  $\kappa$ . The volume probability distribution function of the IMBH population in a given galaxy,  $u(r)$ , is therefore obtained from that for the Milky Way, as  $u(r) = g(r/\kappa)/\kappa^3$ . This procedure has been satisfactorily tested by comparing the results with a limited number of mock catalogs, obtained as an exploratory study in Ref. [20], for different host galaxies masses. The virial radius for a halo of a given mass  $M$  at a given redshift is defined as the radius of a spherical volume within which the mean density is  $\Delta_c(z)$  times the critical density at that redshift,  $M = 4\pi r_{vir}^3 \Delta_c(z) \rho_c(z) / 3$ , with the virial overdensity  $\Delta_c(z)$  as given in Ref. [49].

## B. DM distribution around IMBHs

The process of adiabatic growth of a black hole at the center of a DM mini-halo produces a steepening of the initial DM profile, leading to large DM overdensities called spikes [50]. Interestingly, while for the SMBHs at the center of the galaxies the DM interaction with baryons and dynamical processes tend to weaken the spike [13, 22], these effects are not effective for the dense mini-spikes around IMBHs. Starting from a DM profile with a power law behavior in the proximity of the BH  $\rho \sim r^{-\gamma}$ , the final spike profile after adiabatic growth reads [50]:

$$\rho_{sp}(r) = \rho(r_{sp}) \left( \frac{r}{r_{sp}} \right)^{-\gamma_{sp}}, \quad (1)$$

where  $\rho$  is the density function of the initial profile and the final slope  $\gamma_{sp}$  is given by  $\gamma_{sp} = \frac{9-2\gamma}{4-\gamma}$ , weakly depending on its initial value  $\gamma$ . The radius of the gravitational influence of the black hole  $r_h$  sets a limit within which the spike profile is valid, i.e.  $r_{sp} \approx 0.2r_h$ , where  $r_h$  is implicitly defined as:

$$M(r < r_h) \equiv \int_0^{r_h} \rho(r) r^2 dr = 2M_\bullet,$$

with  $M_\bullet$  is the mass of the black hole [22].

In the simulation of Ref. [20] the authors considered an initial NFW DM density profile, with the average parameters for the spike set as  $r_{sp} = 6.8 \text{ pc}$  and  $\rho_{sp} = 1.2 \cdot 10^{10} M_\odot \text{ kpc}^{-3}$ . We employ here these reference values throughout our analysis.

After the formation of the BH, the DM number density decreases because of DM pair annihilations as:  $\dot{n}_\chi = -(\sigma v)n_\chi$  with  $(\sigma v)$  the annihilation cross section times velocity. The solution to this equation gives an upper limit to the DM density  $\rho_{lim} = m_\chi \times (\sigma v)^{-1} (t - t_f)^{-1}$  where  $m_\chi$  indicates the DM mass and  $t - t_f$  is the time elapsed since BH formation. We denote  $r_{lim}$  the radius where this maximum density is reached. The density is considered to be constant within a cut-radius defined as  $r_{cut} = \text{Max}[4R_{Schw}, r_{lim}]$  where  $R_{Schw}$  is the BH Schwarzschild radius. For the spikes in the simulation

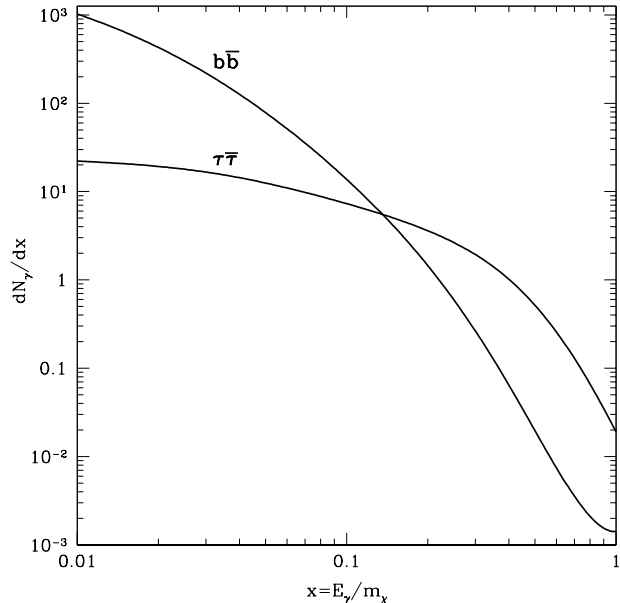


Figure 2: Photon spectra for DM annihilation into  $b\bar{b}$  and  $\tau^+\tau^-$ . The DM particle mass is set to  $m_\chi = 100$  GeV

of Ref. [20], the cut-radius at  $z = 0$  is, averaging over all mini-spikes in the simulation,  $r_{cut} = 5 \times 10^{-3}$  pc, for  $(\sigma v) = 3 \cdot 10^{-26} \text{ cm}^3 \text{ s}^{-1}$ .

### III. COSMIC GAMMA-RAY BACKGROUND

We compute in this Section the mean intensity of the CGB from unresolved mini-spikes and from unresolved blazars. In this and following sections, we use a similar notation to that adopted in Ref. [30].

#### A. Dark Matter Annihilations

##### 1. DM annihilation contribution to cosmic gamma-ray background

Following Ref. [18], the CGB gamma-ray flux from cosmological DM mini-spikes, defined as the number of photons per unit area, time, solid angle and energy, is then obtained as:

$$\langle I(E)_{DM} \rangle = \int dr W(E[1+z], z), \quad (2)$$

where

$$W(E, z) = \frac{(\sigma v)}{8\pi m_\chi^2} \frac{dN_\gamma}{dE}(E[1+z]) e^{-\tau(E[1+z], z)} \Delta^2(z). \quad (3)$$

The absorption of gamma-rays due to interaction with the diffuse extragalactic background light is parametrized

through the effective optical depth  $\tau$  as in Ref. [14]. The comoving distance  $r$  and the redshift  $z$  are interchangeably used and the element  $dr$  is simply  $dr = c/H(z)dz$  with  $H(z)$  the Hubble function. The function  $\Delta^2(z)$  in Eq. (3) is

$$\Delta^2(z) = n(z) \int_{r_{cut}}^{r_{sp}} \rho_{sp}^2(r) d^3r,$$

with  $n(z)$  the comoving number density of IMBHs.

The gamma-ray annihilation spectrum  $dN_\gamma/dE$  depends on the DM particle physics model; i.e., it determines the branching ratios for annihilation in Standard Model final states. Given these branching ratios (which can be computed for any specified particle DM model), the quantity  $dN_\gamma/dE$  can be reconstructed via Monte Carlo simulations. This is how, for instance,  $dN_\gamma/dE$  is computed in codes like `DarkSUSY` [51] which, in particular, makes use of `Pythia` [52, 53] Monte Carlo simulations.

From the discussion above, it is clear that the specific DM annihilation spectrum depends critically on the particle physics model. In the present study we wish to consider a particle dark matter setup as model independent as possible. As such, we consider two representative standard model final states, and assume that the DM particle annihilates 100% of the time in one of those two final states. For definiteness, we consider the final states  $b\bar{b}$  and  $\tau^+\tau^-$ . The choice is motivated by both theoretical and phenomenological considerations: first, in the context of supersymmetry, perhaps the best motivated extension to the standard model encompassing a DM candidate, these final states are ubiquitous; second, the resulting DM annihilation spectra  $dN_\gamma/dE$  cover the two extreme cases of a soft photon spectrum ( $b\bar{b}$ ) and of a relatively hard spectrum ( $\tau^+\tau^-$ ). Even harder photon spectra are in principle possible, for instance in the context of universal extra dimensions [4], or in other models with a large branching ratio in charged leptons. This is not critical to us, since we only focus on a single gamma-ray energy in our analysis; our results for the  $\tau^+\tau^-$  are conservative with respect to even harder photon spectra, and the comparison with the soft spectrum we picked is a solid guideline to what would change with an even harder spectrum.

In supersymmetry, in the large  $\tan\beta$  regime favored by Higgs searches at LEP, the dominant annihilation final states for the lightest neutralino include gauge bosons (if kinematically open) and down-type fermion-antifermion final states. The role of gauge bosons depends on the higgsino fraction of the lightest neutralino. Supersymmetric models with radiative electroweak symmetry breaking and gaugino unification at the grand unification scale feature generically a small higgsino fraction. In any case, the spectrum resulting from gauge boson final states resembles closely the  $b\bar{b}$  spectrum [3, 54, 55]. If down-type fermion-antifermion final states dominate, pair annihilation into  $b\bar{b}$  is the dominant channel, possibly competing with  $\tau^+\tau^-$  but winning over it by a factor 3 from color

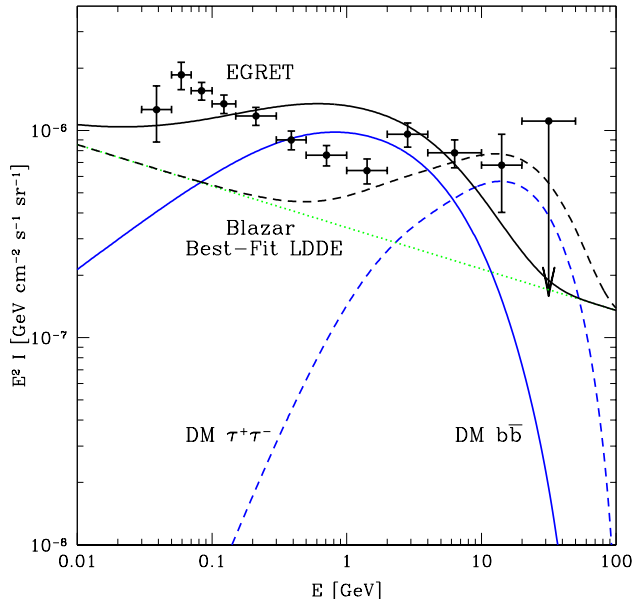


Figure 3: Cosmic gamma-ray background spectrum from DM annihilation in mini-spikes (dashed) and blazars with the best fit LDDE GLF model(dotted). The sum of the two signals is shown as a solid line and the data points are from EGRET data [58].

and by the square of the bottom-to-tau mass ratio (see e.g. [56]). In some cases, however, supersymmetry predicts a large branching ratio in  $\tau^+\tau^-$ , for instance when the lightest neutralino relic abundance is driven by coannihilation with the lightest stau, which then also mediates the dominant pair-annihilation channel. Several supersymmetric models feature  $\tau^+\tau^-$  as the dominant annihilation channel. In addition, other models [4] where for instance the quantum numbers of the DM particle weigh favorably charged leptons over quarks, naturally feature a hard photon spectrum, close to  $\tau^+\tau^-$ .

In summary, in the present study we restrict ourselves to the two final states  $b\bar{b}$  and  $\tau^+\tau^-$  as representative WIMP annihilation final states bracketing a wide range of model-dependent predictions. The input spectra, shown in Fig. 2, are the results of the numerical study of Ref. [57].

## 2. Modeling the mini-spikes number density

The IMBH number density is parametrized following the numerical study of Ref. [47]. We consider that one IMBH is formed at redshift  $z_{re}$  in every DM halo with a mass higher than  $M_{min} = 10^8 M_\odot$ . As mentioned in Sec. II, IMBHs cannot be formed at more recent epochs and the formation at higher redshifts is negligible. In any case, the prescription we have adopted provides a lower limit to the CGB mean flux from mini-spikes, also

in view of the fact that more than one IMBH could be formed in larger halos as well.

The comoving number density at the formation redshift, is obtained as:

$$n(z_{re}) = \int_{M_{min}}^{\infty} dM \frac{dn}{dM}(M, z = z_{re}). \quad (4)$$

We employ here the halo mass function  $dn/dM(M, z)$  given in Ref. [59], with the transfer function of Ref. [60].

After formation, IMBHs get redistributed in halos during their hierarchical mergers. At the present epoch, the comoving number density of unmerged IMBHs is given by:

$$n(0) = \int_{M_{min}}^{\infty} dM \frac{dn}{dM}(M, z = 0) N_{bh} \frac{M}{10^{12.1} h^{-1} M_\odot}, \quad (5)$$

with the average number of IMBHs in the Milky Way halo  $N_{bh}$  obtained from the simulation of Ref. [47]. Here we assume a linear dependence of the number of unmerged IMBHs on their host halo mass. As noticed in Ref. [18], reasonable deviations from the this linear interpolation produce small changes on the final CGB flux.

At intermediate redshift, we follow the prescription of Ref. [18], and compute  $n(z)$  assuming a redshift power-law behavior, with the index  $\beta$  obtained by fitting  $n(z)$  at  $z = 0$  and  $z = z_f$ :

$$n(z) = n(z_f) \left( \frac{1+z}{1+z_f} \right)^\beta. \quad (6)$$

Reference [47] found that a Milky-Way like galaxy would host a population of  $N_{sp} = 101$  IMBHs at  $z = 0$ . For the same choice of the cosmological parameters and using Eqs. (11) and (6) we obtain  $\beta = 0.3$ , as in Ref. [18]. This computation can be updated by using the more precise measurements of the cosmological parameters from WMAP5 [35]. Keeping  $\beta = 0.3$ , we obtain a sensible decrease of the IMBH number density and for a Milky-Way like halo at  $z=0$ , we get  $N_{sp} = 40$ .

For the rest of the paper we will therefore assume  $N_{sp} = 40$  and  $\beta = 0.3$  to parametrize the IMBH number density. Using Eq. (2) we can now compute the mean extragalactic gamma-ray flux from DM annihilation in cosmological mini-spikes. The integration over  $z$  is performed up to the formation redshift, i.e.,  $z_{re}$ . The results are shown in Fig. 3 adopting  $m_\chi = 100$  GeV and  $\langle\sigma v\rangle = 3 \times 10^{-26} \text{ cm}^3 \text{ s}^{-1}$  and for DM annihilation into  $b\bar{b}$  and  $\tau^+\tau^-$ . In the same plot are shown the measurements of the CGB extracted from EGRET data [58]. The predictions largely depend on the annihilation spectrum, with the CGB flux peaking at higher energies for harder spectra. For energies of the order  $\mathcal{O}(1-10)$  GeV, the contribution from DM annihilation is at the same level of the CGB intensity inferred from EGRET measurement, suggesting therefore that in this energy range DM annihilation could substantially contribute to the total CGB flux.

In our analysis, we have included also the contribution from low redshifts, where IMBHs are potentially detectable. Previous studies have shown that the Fermi satellite is expected to resolve mini-spikes in our galaxy [20] and maybe Andromeda [26] but not further. On the other hand, the contribution of IMBHs from  $z < 10^{-5}$  to the extragalactic gamma-ray background is negligible.

## B. Unresolved Blazars

The gamma-ray luminosity function (GLF) of blazars is obtained from the luminosity dependent density evolution (LDDE) model of Ref. [61].

The CGB flux from unresolved blazar is computed as:

$$E \langle I_B(E) \rangle = \int_0^{z_{max}} dz \frac{d^2 V}{dz d\Omega} \int_{L_{min}}^{L_{max}(z)} dL \rho_\gamma(L, z) \mathcal{F}_E(L, z).$$

The functions in the Equation above are derived in Ref. [30] and references therein. The minimum blazar luminosity is taken to be  $L_{min} = 10^{41}$  erg s $^{-1}$  and the EGRET flux sensitivity above 100 MeV is  $10^{-7}$  cm $^{-2}$  s $^{-1}$ . In Fig. 3 we show the results for the best-fit LDDE GLF model (details on the blazar model can be found in Ref. [30]).

## IV. COSMIC GAMMA-RAY ANGULAR CORRELATIONS

### A. Dark Matter Annihilations

The angular power spectrum  $C_l$  of the CGB from DM annihilation in substructures has been computed in Ref. [30]. Here we adapt their formalism to the case of mini-spikes and we refer to the original reference for the derivation of the equations.

The angular power spectrum from mini-spikes is obtained as:

$$\langle I(E) \rangle^2 C_l = \int \frac{dr}{r^2} W([1+z]E, z)^2 P_{DM} \left( \frac{l}{r}, z \right), \quad (7)$$

where  $P_{DM}(k)$  is the spatial power spectrum of mini-spikes and it can be divided into 1-halo and 2-halo terms:

$$P_{DM}(k) = P^{1h}(k) + P^{2h}(k), \quad (8)$$

$$P^{1h}(k) = \int_{M_{min}}^{\infty} dM \frac{dn}{dM} \left( \frac{\langle N|M \rangle}{n(z)} \right)^2 |u(k, M)|^2, \quad (9)$$

$$P^{2h}(k) = \left[ \int_{M_{min}}^{\infty} dM \frac{dn}{dM} \frac{\langle N|M \rangle}{n(z)} b(M) |u(k, M)| \right]^2 \times P^{linear}(k, z). \quad (10)$$

These terms refer to correlations between two points in the same halo (1-halo) or in two different halos (2-halo).

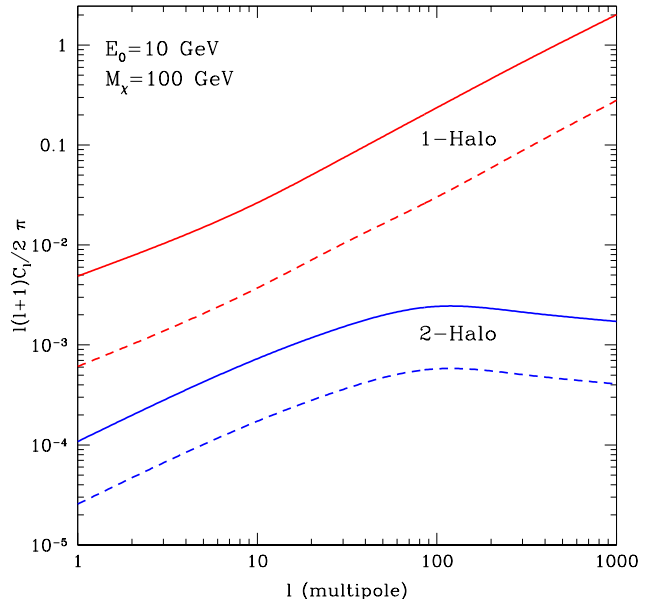


Figure 4: Angular power spectrum from DM annihilation in mini-spikes computed at  $E_0 = 10$  GeV. We show separately the contributions from 1-halo (red) and 2-halo (blue) terms. The total angular power spectrum is the sum of the two curves. Solid lines refer to DM annihilation into  $b\bar{b}$  and dashed ones are for  $\tau^+\tau^-$  final states. We set the DM particle mass to  $m_\chi = 100$  GeV.

The function  $u(k, M)$  is the Fourier transform of the IMBH volume probability, defined in Sec. II. The linear power spectrum  $P(k)$  is obtained using the transfer function of Ref. [60] and the bias parameter is taken from Ref. [62].

The function  $\langle N|M \rangle$  gives the number of IMBHs in a halo of given mass at a given redshift and it is related to the IMBH comoving number density as:

$$n(z) = \int_{M_{min}}^{\infty} dM \frac{dn}{dM} \langle N|M \rangle. \quad (11)$$

As noticed in Sec. II, at  $z = 0$   $\langle N|M \rangle$  is well approximated by  $\langle N|M \rangle_{lin} = N_{sp} \left( \frac{M}{10^{12.1} h^{-1} M_\odot} \right)$  with  $N_{sp}$  corresponding to  $N_{sp} = 40$ , as appropriate for the Milky Way. On the other hand, at the formation redshift we assume that one BH is formed for every halo with mass above  $M_{min}$ . Formally, there is no unique expression for  $\langle N|M \rangle$  which interpolates the two regimes above and that, at the same time, allows one to reproduce Eq. (6) from Eq. (11). We have explored different parametrization for  $\langle N|M \rangle$  encompassing its limiting behaviors at  $z = 0$  and  $z = z_{re}$  and overestimating and underestimating  $n(z)$  with respect to Eq. (6). Since the power spectrum computed in Eq. (7) is dominated by the contribution at small  $z$ , we have found that these different choices produce differences in  $C_l$  always between a factor 2, that are within other uncertainties in the calculations. This is also true



also for the cross-correlation terms that we will introduce in Sec. V.

From Eq. (7), we note that the multipoles  $C_l$  are independent of the value of  $(\sigma v)$  and of the choice of DM density profile around each IMBH. We also find that they are weakly dependent on the normalization  $N_{bh}$ .

In Fig. 4 we show, for the two different WIMP annihilation channels, the contributions of 1-halo and 2-halo terms on the angular power spectrum. We picked a gamma-ray energy at which we compute the anisotropy power spectrum of  $E = 10$  GeV, and fixed the particle DM mass to  $m_\chi = 100$  GeV.

The 2-halo term turns out to be negligible at all angular scales. The slope of the 1-halo term lies between those of the 1-halo terms for annihilation in subhalos and smooth NFW halos computed in Ref. [30] (see their Fig. 2). This can be understood considering that the signal in the subhalo- and in the smooth-halo-dominated cases follow respectively the density profile and its square and for the case of a NFW profile the two distributions are respectively steeper and shallower than the IMBH radial distribution. The increased normalization of the power spectrum with respect to the case of subhalos emission is explained by the same argument: the Fourier transform of the IMBH profile gets more power at high  $k$  with respect to that of NFW. The same tendency is found for the two choices of the annihilation spectra. The angular power spectrum for DM annihilation into  $b\bar{b}$  is larger than that for  $\tau^+\tau^-$  final states because at the energy of  $E_0 = 10$  GeV, the former photon spectrum is significantly steeper than the latter.

## B. Blazars

The angular power spectrum from unresolved blazar comes from the contributions of a Poisson term  $C_l^P$  and a correlation term  $C_l^C$ , respectively the 1-halo and 2-halo terms:

$$C_l = C_l^P + C_l^C, \quad (12)$$

$$C_l^P = \frac{1}{E^2 \langle I_B(E) \rangle^2} \int dz \frac{dV}{dz d\Omega} \times \int_{L_{min}}^{L^{max}(z)} dL \rho_\gamma(L) \mathcal{F}_E(L, z)^2, \quad (13)$$

$$C_l^C = \frac{1}{E^2 \langle I_B(E) \rangle^2} \int dz \frac{dV}{dz d\Omega} P_{lin} \left( \frac{l}{r(z)} \right) \times \left[ \int_{L_{min}}^{L^{max}(z)} dL \rho_\gamma(L) b_B(L, z) \mathcal{F}_E(L, z) \right]^2. \quad (14)$$

The blazar bias  $b_B$  indicates how strong blazars are clustered with compared to the linear matter power spectrum. Presently, this value is uncertain, and different (generically inconsistent) estimates are inferred from different techniques. Current observations give an upper bound  $b_B \lesssim 5$  (see Ref. [61]).

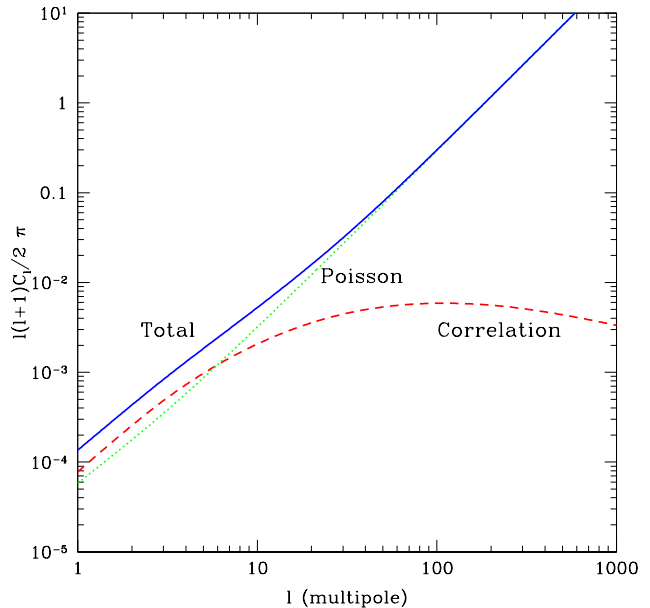


Figure 5: Angular power spectrum of the CGB from unresolved blazars expected for Fermi. We show separately the Poisson (dotted) and the correlation (dashed) terms. The total is simply the sum, and is shown as a solid curve. We assume here the best-fit LDDE GLF model.

Reference [30] estimated the correlation term assuming either a bias model inferred from quasar observations or a simply constant  $b_B = 1$ . The results obtained are quite similar since the main contribution to the CGB comes from low-redshift blazars, which have bias close to 1. In addition, for  $l \gtrsim 10$  the total angular power spectrum is dominated by the Poisson term.

We present in Fig. 5 our predictions for the angular power spectrum expected to be reconstructed from Fermi data, adopting the best-fit LDDE GLF model. We assume a Fermi point source sensitivity of  $2 \times 10^{-9} \text{ cm}^{-2} \text{ s}^{-1}$ , the value expected for energies above  $E = 100$  MeV and two years of full sky survey mode, for sources with a spectral index equals to 2. We note that the power spectrum is independent of the gamma-ray energy, since we have assumed the same power-law spectrum for all blazars and these dependence exactly cancels when we divide by the mean intensity squared in Eq. (13) and Eq. (14).

## V. DISTINGUISHING DARK MATTER ANNIHILATION FROM BLAZARS

We outline here the prospects for distinguishing DM annihilation from blazar emissions in the angular power spectrum of CGB with Fermi.

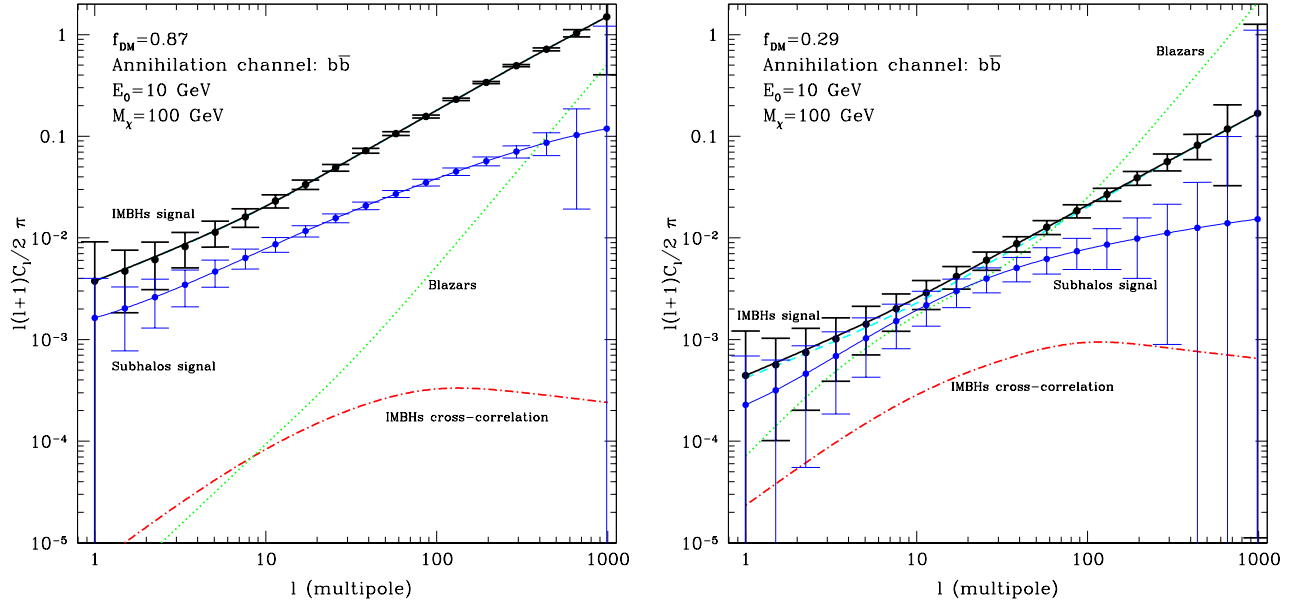


Figure 6: Angular power spectrum of the CGB from DM annihilations around IMBHs at a photon energy  $E_0 = 10$  GeV. Dashed line shows the contribution from DM annihilation ( $f_{DM}^2 C_l^{DM}$ ), dotted line is for blazars ( $f_B^2 C_l^B$ ) and the dot-dashed line is the cross-correlation term  $2f_{DM}f_B C_l^{Cr}$ . The total signal  $C_l^s$  is shown as a thick black solid curve. Error bars are for 2-years of Fermi data. The thin blue solid curve show the DM signal for DM annihilations in subhalos [30] (see text for more details).

### A. Angular correlations of CGB in the two component case

The CGB background receives contributions from both DM annihilation and from ordinary astrophysical sources, with unresolved blazars being a representative candidate for the latter class of emitters. For the detection of DM annihilation in the CGB, blazars therefore constitute a background. Their contribution is currently uncertain but we expect it will be modeled rather precisely with the Fermi catalog of detected blazars. In addition, as mentioned in Sec. IV the angular power spectrum for astrophysical sources is energy independent and therefore it could be calibrated at low energies where the contribution from DM annihilation is negligible and then subtracted from the total anisotropy data. For this analysis we therefore treat the blazar contribution as a known background, and we study the prospects for detecting DM annihilation on top of it.

In this two component analysis, the total CGB intensity is the sum of the DM and blazar contributions:

$$\langle I_{CGB}(E) \rangle = \langle I_{DM}(E) \rangle + \langle I_B(E) \rangle.$$

Labeling with  $f_{DM}$  the fraction of the total CGB coming from DM annihilation,  $f_{DM} = \langle I_{DM}(E) \rangle / \langle I_{CGB}(E) \rangle$ , the total angular power spectrum is:

$$C_l^{CGB} = f_{DM}^2 C_l^{DM} + 2f_{DM}f_B C_l^{Cr} + f_B^2 C_l^B,$$

where  $C_l^{DM}$  and  $C_l^B$  are respectively the angular power

spectrum from DM annihilation and blazars and  $f_B$  is simply  $f_B = 1 - f_{DM}$ .

The cross-correlation term  $C_l^{Cr}$  has been studied in Ref. [30] and is divided into 1-halo and 2-halo terms:

$$C_l^{Cr,1-halo} = \frac{W([1+z]E, z)}{E \langle I_B(E) \rangle \langle I_{DM}(E) \rangle} \int_{L_{min}}^{L^{max}(z)} dL \rho_\gamma(L) \times \mathcal{F}_E(L, z) \frac{\langle N|M \rangle}{n(z)} u\left(\frac{l}{r}, M[L]\right), \quad (15)$$

$$C_l^{Cr,2-halo} = \frac{W([1+z]E, z)}{E \langle I_B(E) \rangle \langle I_{DM}(E) \rangle} \int_{L_{min}}^{L^{max}(z)} dL \rho_\gamma(L) \times \mathcal{F}_E(L, z) b_B(L, z) \int_{M_{min}}^{\infty} \frac{dn(M, z)}{dz} \frac{\langle N|M \rangle}{n(z)} \times b(M, z) u\left(\frac{l}{r}, z, M\right) P_{lin}\left(\frac{l}{r}, z\right). \quad (16)$$

A relation between the blazar luminosity and its host halo mass,  $M[L]$  is given in Ref. [61].

In this two component framework, the total signal  $C_l^s$  and the background noise  $C_l^b$  therefore read:

$$C_l^s = f_{DM}^2 + 2f_{DM}(1 - f_{DM})C_l^{Cr}, \quad (17)$$

$$C_l^b = (1 - f_{DM})^2 C_l^B. \quad (18)$$

The GLF-LDDE blazar model in Ref. [61] basically depends on three parameters ( $\gamma_1, q, k$ ) and as reminded in Sec. III, the best-fit model only accounts for  $\sim 15\%$  of the CGB intensity at 10 GeV. However, varying the



parameters of the blazar model allows to explain different fractions of the CGB. For example setting them to ( $\gamma_1 = 1.36$ ,  $q = 3.80$ ,  $k = 3.15 \times 10^{-6}$ ) we obtain a blazar fraction  $f_B = 0.71$ . On the other hand, the contribution from DM annihilation in mini-spikes is largely affected by astrophysical and particle physics uncertainties. For example, in WIMP models the mass usually lies in the broad range  $\mathcal{O}(1-1000)$  GeV<sup>1</sup> and  $(\sigma v)$  can largely differ from the thermal value  $(\sigma v) = 3 \times 10^{-26}$  cm<sup>3</sup> s<sup>-1</sup> in the presence of efficient coannihilations or Sommerfeld corrections, if the DM candidate is nonthermally produced or if a modified cosmological expansion rate is postulated at the time of WIMP freeze-out. Moreover, as discussed in Sec. III, the number of mini-spikes in halos could differ from that found in simulations, since IMBH formation could have been underestimated or on the contrary IMBHs could have been more efficiently destroyed by astrophysical processes than what is expected. In addition, the DM density profile around each IMBH could be modified as well by feedback.

Motivated by these arguments we compute two different models of blazars, explaining respectively a small and an high fraction of the CGB at 10 GeV, and we assume that the remaining CGB intensity comes from DM annihilation in mini-spikes. As a benchmark model we fix the DM mass to  $m_\chi = 100$  GeV and we refer to annihilation to  $b\bar{b}$  pairs. Following Ref. [30], we choose an energy of observation  $E_0 = 10$  GeV as a compromise between maximization of signal count and minimization of the Galactic emission. At lower energies, the galactic foreground becomes stronger, masquerading the extragalactic component, while at higher energies, the photon count is more suppressed. However, we perform our analysis also for different choices of DM parameters and energies of detection.

## B. Prospect for detection with the Fermi Telescope

The Large Area Telescope (LAT) onboard the Fermi satellite is currently taking scientific data in a survey mode. The LAT has a more than one order of magnitude better sensitivity in the 20 MeV to 10 GeV region than its predecessor Energetic Gamma Ray Experimental Telescope (EGRET) onboard the Compton Gamma-ray Observatory [64]. In addition, the LAT extends the high-energy gamma-ray region up to around 300 GeV. In the present study, we consider a mean exposure of  $1.2 \times 10^{11}$  cm<sup>2</sup> s, corresponding, roughly, to 2 years of all-sky survey mode operation [65, 66, 67]. We assume an angular resolution for 68% containment of the point spread function of  $\sigma_b = 0.115^\circ$ , appropriate for energies of around 10 GeV. Our choices reflect those described

in Ref. [30]. The angular resolution improves at larger energies, and degrades at lower energies.

For the type of study hereby presented, a thorough knowledge of the gamma-ray galactic background will be warranted. In addition, disentangling the diffuse extragalactic background from the mentioned galactic emission will also be challenging. Realistically, the 2 years of observations we consider refer not to the early stages of the mission but, rather, to a stage when these backgrounds are considered to be thoroughly under control.

Considering the Fermi specifications described above, the projected 1- $\sigma$  error bars of the CGB power spectrum from DM annihilation is:

$$\delta C_l^s = \sqrt{\frac{2}{(2l+1)\Delta l f_{sky}}} \left( C_l^s + C_l^b + \frac{C_N}{W_l^2} \right). \quad (19)$$

We take a bin width  $\Delta l = 0.5l$ . The window function of a gaussian point spread function is  $W_l = \exp(-l^2 \sigma_b^2/2)$ .  $C_N$  is the photon spectrum of the photon noise and it is given by  $C_N = \Omega_{sky} N_{tot}/N_{CGB}^2$  with  $N_{tot}$  and  $N_{CGB}$  respectively the total and CGB photon numbers detected from a region of sky  $\Omega_{sky}$ .

Following Ref. [30], we restrict the analysis to galactic latitudes  $|b| > 20^\circ$ . At lower latitudes, the galactic foreground dominates over the CGB flux, while the situation is expected to be reversed in the region we consider. After the cut of the galactic plane, the fraction of sky we consider is  $f_{sky} = 0.66$ . Using  $N_{tot} \sim N_{CGB}$  we obtain  $C_N \sim 4\pi f_{sky}/N_{CGB} = 8 \times 10^{-5} (E/10 \text{ GeV})$ . Here we employ the total CGB flux as estimated from EGRET data. We note, however, that since Fermi is expected to detect a large number of blazars, the total GCB intensity will be in all likelihood reduced, possibly lowering our error estimations.

In Fig. 6, we present our predictions for two blazar models contributing a fraction  $f_B = 0.13$  and  $f_B = 0.71$  of the total CGB flux at  $E_0 = 10$  GeV. We show the signal and the background power spectra that Fermi is expected to measure after two years of observations as well as the projected 1- $\sigma$  signal error bars. The signal is detected if  $C_l^s > \delta C_l^s$ . We notice that this occurs even if the DM contribution is very small. In addition, the shape of the DM power spectrum is very different from the one corresponding to blazars. This feature could therefore help distinguish the two scenarios.

In Refs. [29, 30], the authors first studied the angular anisotropies of the CGB from DM annihilation. They focused their attention on two scenarios, the first assuming that the DM signal is dominated by annihilations occurring in cosmological DM halos and the latter considering that the dominant contribution comes from the populations of DM clumps hosted in the main DM halos. For each possibility they took into account the possible uncertainties on the minimum halo mass value and on the halo occupation distribution, i.e., the number of subhalos in a parent halo of given mass. For these frameworks, they computed the angular power spectrum from DM

<sup>1</sup> For a recent discussion of ultra-light WIMPs in supersymmetry see Ref. [63].

annihilation that Fermi is expected to measure. They concluded that provided DM annihilation contribute to the CGB at 10 GeV with a fraction  $f_{DM} \gtrsim 0.3$ , after two years of data taking Fermi will be able to detect the DM signal.

In Fig. 6, we show their results for the most promising case, i.e., when the DM signal is dominated by cosmological clumps with an halo occupation distribution  $\langle N|M \rangle \propto M$ . We consider that DM annihilations in subhalos contribute to a certain fraction  $f_{DM}$  to the CGB intensity at 10 GeV and the remaining flux comes from blazars. In each plot the DM fraction  $f_{DM}$  is the same for the mini-spike and clump scenarios. The signal for the subhalo case with the associated  $1\text{-}\sigma$  error bars is plotted as a thin blue solid line. Comparing the DM signals in the mini-spike and subhalos scenarios we notice that provided that DM annihilations largely contribute to the CGB mean intensity, there are promising prospects for distinguish the two cases. This conclusion is further strengthened if we consider DM annihilation in cosmological smooth halos instead of clumps, since, as stated before, the expected angular power spectrum is smaller than when subhalos emission dominates.

### C. Power spectrum dependence on energy of detection, annihilation spectrum and DM mass.

Even if the results discussed in the section above refer to a certain specific choice of DM parameters and energy of detection, we have also repeated the calculations for different cases. Rather than presenting all the plots, we just show in Fig. 7 what we obtained for some benchmarks and we try to summarize some general guidelines. A more complete analysis, for example dedicated to the optimization of the energy of detection as a function of the particle mass, is beyond the scope of this study.

First we show how our predictions change if we pick another energy of detection. At energies higher than 10 GeV the galactic foreground is sensibly suppressed but also the photon number from DM annihilation is reduced, since the interval of integration in energy is shrunk. Therefore, it is not trivial to infer which is the effect on the DM angular power spectrum and its error bars. We find that even if the CGB mean intensity at 20 GeV is reduced with respect to its value at 10 GeV, the power spectrum is increased. We remind that the power spectrum is normalized to the mean flux, as in Eq. (7). At an energy of 1 GeV the CGB mean intensity is comparable with the galactic foreground therefore in Eq. (19) we consider  $C_N \sim 2\Omega_{sky}/N_{CGB}$ . For this gamma-ray energy, the signal is sensibly reduced and the prospects for detection are degraded.

As pointed out in Sec. IV for softer energy spectra, the normalization of angular power spectrum is decreased. We indeed find this behavior when we compare the results obtained for the  $\tau^+\tau^-$  and for the  $b\bar{b}$  DM annihilation final states. For the ‘‘pessimistic’’ case of annihila-

tions into  $\tau^+\tau^-$ , assuming an energy of detection of 10 GeV and  $m_\chi = 100$  GeV, DM annihilations have to contribute at least with a fraction  $f_{DM} \sim 0.3$  to the mean CGB in order to be detectable in the CGB angular power spectrum with Fermi.

We finally show the results for  $m_\chi = 1000$  GeV and  $E_0 = 10$  GeV. The photon spectra from DM annihilation can in good approximation be scaled with the particle mass defining the adimensional variable  $x = E/m_\chi$ , as in Fig. 2. Therefore, looking at Eq. (3) and Eq. (7), we note that there is an approximate scaling which links the angular power spectra computed at different energies of observations and for particle of different masses. For example, the choices ( $E_0 = 10$  GeV,  $m_\chi = 1000$  GeV) and ( $E_0 = 1$  GeV,  $m_\chi = 100$  GeV) actually correspond to the same value of  $dN_\gamma/dx$ , and should thus lead to identical angular power spectra. This scaling is broken by the dependence of the function  $\tau(z)$  on  $E_0$  in Eq. (3), which fortunately is not important at the energies of interest, and our qualitative considerations are still roughly valid. This can be seen noting that the power spectra in Fig. 7 for the two cases above are indeed very similar. Note however that, as already stressed, different energies of observations significantly affect the projected errors bars.

## VI. CONCLUSIONS

DM annihilation in mini-spikes around IMBHs is a promising scenario for indirect DM searches with gamma rays. In particular, Fermi is expected to detect a significant fraction of the IMBH population in the Milky Way and maybe a few sources in the Andromeda galaxy. The remaining cosmological mini-spikes will remain unresolved, but could leave their imprint in the CGB. As shown in [18], for a standard neutralino with a mass  $m_\chi = 100$  GeV and a ‘‘thermal’’ annihilation cross section  $(\sigma v) = 3 \cdot 10^{-26} \text{ cm}^3\text{s}^{-1}$  the predicted CGB flux from cosmological mini-spikes is comparable to the EGRET CGB flux at gamma-ray energies of  $\mathcal{O}(1 - 10)$  GeV. We find that, for example, this corresponds to a fraction  $f_{DM} = 0.35$  and  $f_{DM} = 0.72$  of the CGB at  $E = 10$  GeV, respectively for DM annihilation into  $b\bar{b}$  and  $\tau^+\tau^-$ . Fermi is expected to resolve a much larger number of galactic and extragalactic gamma-ray sources compared to its predecessor EGRET, with the expectation of reducing the measured unresolved diffuse CGB flux. At the same time, only IMBHs very close to us will be resolved, therefore the DM contribution to the CGB could be increased with respect to our estimates, based on the mean CGB spectrum extracted from EGRET data.

However, in absence of characteristic spectral features, it will be problematic to distinguish DM annihilation and ordinary astrophysical emissions from the mean GCB intensity. Instead, Ref. [30] showed that gamma-ray anisotropy data could provide a more suitable tool to pursue this program. In fact, provided DM annihilation

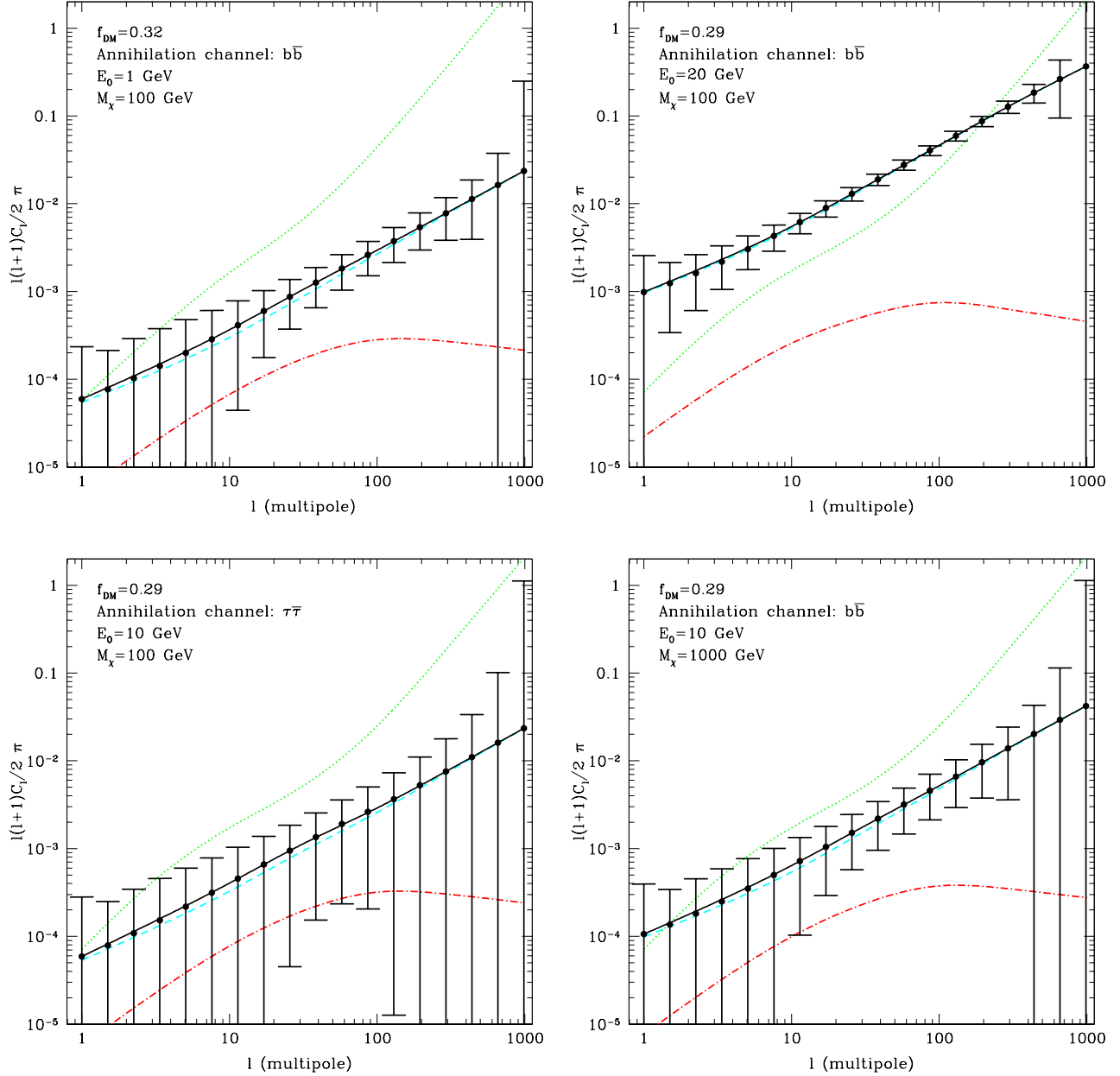


Figure 7: Angular power spectrum of the CGB from DM annihilation and for blazars. Lines are as in Fig. 6. Annihilation channel, energy of detection, DM mass and fractional contribution to the CGB mean intensity are specified for each panel.

contributes substantially to the CGB mean intensity, it will be detectable in the CGB angular power spectrum by Fermi.

Motivated by these considerations, in this paper, we studied the anisotropies of the CGB in the mini-spikes scenario. Astrophysical and particle physics uncertainties largely affect the predictions for the mean CGB intensity from mini-spikes and also the blazar contribution is currently unknown. Considering these two sources as the main components of the CGB, we computed their angular power spectra for different relative contributions

and, treating the blazar component as a known background, we studied the prospects for DM annihilation detection in the CGB angular power spectrum with two years of Fermi observations. We expect that considering unresolved blazars as a background is a reasonable assumption, since their GLF and bias should be quite reliably reconstructed from the Fermi source catalog.

We repeated our computations for different detection energies, particle masses and annihilation modes, showing that our results are significantly affected by all these parameters. Interestingly, this could mean that informa-

tion on these three quantities can actually be inferred from the measured DM-induced gamma-ray anisotropy power spectrum. However a more detailed analysis would be necessary to fully study the potential of the anisotropy technique to reconstruct these parameters. We found that the shape of the DM power spectrum is very different from that of blazars, providing a robust handle to disentangle the two signals. Astrophysical sources other than blazars could however also contribute to the CGB and, if spatially extended, as clusters of galaxies, the shape of their angular power spectrum could significantly differ from that of blazars, which is dominated at large multipoles by the Poisson term. We stress that even in this case we could calibrate the astrophysical power spectrum at low energies, where DM annihilations are negligible and subtract it from the measured total CGB power spectrum at the energies of interest. In fact, for sources with power-law energy spectra, the gamma-ray angular power spectrum is energy independent and this condition is common to almost any class of standard astrophysical

gamma-ray emitter.

In conclusion, we showed that the prospects for detecting DM annihilation from cosmological mini-spikes in the angular CGB power spectrum with Fermi are promising, and that the analysis of the anisotropy power spectrum allows not only a discrimination of a DM component against astrophysical sources, but also a better understanding of the structures where the DM signal originates.

### Acknowledgments

MT thanks the California Institute of Technology for hospitality and partial support during the preparation of this work. SA is supported by the Sherman Fairchild Foundation. SP is supported by the US Department of Energy under grant DE-FG02-04ER41268 and by the National Science Foundation.

- 
- [1] G. Jungman, M. Kamionkowski, and K. Griest, *Phys. Rept.* **267**, 195 (1996), hep-ph/9506380.
  - [2] L. Bergstrom, *Rept. Prog. Phys.* **63**, 793 (2000), hep-ph/0002126.
  - [3] G. Bertone, D. Hooper, and J. Silk, *Phys. Rept.* **405**, 279 (2005), hep-ph/0404175.
  - [4] D. Hooper and S. Profumo, *Phys. Rept.* **453**, 29 (2007), hep-ph/0701197.
  - [5] O. Adriani et al. (PAMELA) (2008), 0810.4995.
  - [6] J. Chang et al. (ATIC), *Nature* **456**, 362 (2008).
  - [7] G. Bertone, M. Cirelli, A. Strumia, and M. Taoso (2008), 0811.3744.
  - [8] P. Sreekumar et al. (EGRET), *Astrophys. J.* **494**, 523 (1998), astro-ph/9709257.
  - [9] T. Narumoto and T. Totani, *Astrophys. J.* **643**, 81 (2006), astro-ph/0602178.
  - [10] H. Liang, V. Dogiel, and M. Birkinshaw, *Mon. Not. Roy. Astron. Soc.* **337**, 567 (2002), astro-ph/0208509.
  - [11] Y. Rephaeli, J. Nevalainen, T. Ohashi, and A. M. Bykov (2008), 0801.0982.
  - [12] V. Pavlidou and B. D. Fields, *Astrophys. J.* **575**, L5 (2002), astro-ph/0207253.
  - [13] P. Ullio, H. Zhao, and M. Kamionkowski, *Phys. Rev.* **D64**, 043504 (2001), astro-ph/0101481.
  - [14] L. Bergstrom, J. Edsjo, and P. Ullio, *Phys. Rev. Lett.* **87**, 251301 (2001), astro-ph/0105048.
  - [15] J. E. Taylor and J. Silk, *Mon. Not. Roy. Astron. Soc.* **339**, 505 (2003), astro-ph/0207299.
  - [16] D. Elsaesser and K. Mannheim, *Phys. Rev. Lett.* **94**, 171302 (2005), astro-ph/0405235.
  - [17] S. Ando, *Phys. Rev. Lett.* **94**, 171303 (2005), astro-ph/0503006.
  - [18] S. Horiuchi and S. Ando, *Phys. Rev.* **D74**, 103504 (2006), astro-ph/0607042.
  - [19] T. Oda, T. Totani, and M. Nagashima, *Astrophys. J.* **633**, L65 (2005), astro-ph/0504096.
  - [20] G. Bertone, A. R. Zentner, and J. Silk, *Phys. Rev.* **D72**, 103517 (2005), astro-ph/0509565.
  - [21] D. Merritt, M. Milosavljevic, L. Verde, and R. Jimenez, *Phys. Rev. Lett.* **88**, 191301 (2002), astro-ph/0201376.
  - [22] G. Bertone and D. Merritt, *Phys. Rev.* **D72**, 103502 (2005), astro-ph/0501555.
  - [23] E.-J. Ahn, G. Bertone, and D. Merritt, *Phys. Rev.* **D76**, 023517 (2007), astro-ph/0703236.
  - [24] G. Bertone, *Phys. Rev.* **D73**, 103519 (2006), astro-ph/0603148.
  - [25] P. Brun, G. Bertone, J. Lavalle, P. Salati, and R. Taillet, *Phys. Rev.* **D76**, 083506 (2007), 0704.2543.
  - [26] M. Fornasa, M. Taoso, and G. Bertone, *Phys. Rev.* **D76**, 043517 (2007), astro-ph/0703757.
  - [27] M. Fornasa and G. Bertone, *Int. J. Mod. Phys.* **D17**, 1125 (2008), 0711.3148.
  - [28] F. Aharonian et al. (HESS), *Phys. Rev.* **D78**, 072008 (2008), 0806.2981.
  - [29] S. Ando and E. Komatsu, *Phys. Rev.* **D73**, 023521 (2006), astro-ph/0512217.
  - [30] S. Ando, E. Komatsu, T. Narumoto, and T. Totani, *Phys. Rev.* **D75**, 063519 (2007), astro-ph/0612467.
  - [31] A. Cuoco, J. Brandbyge, S. Hannestad, T. Haugboelle, and G. Miele, *Phys. Rev.* **D77**, 123518 (2008), 0710.4136.
  - [32] J. M. Siegal-Gaskins, *JCAP* **0810**, 040 (2008), 0807.1328.
  - [33] D. Hooper and P. D. Serpico, *JCAP* **0706**, 013 (2007), astro-ph/0702328.
  - [34] S. K. Lee, S. Ando, and M. Kamionkowski (2008), 0810.1284.
  - [35] J. Dunkley et al. (WMAP) (2008), 0803.0586.
  - [36] M. C. Miller and E. J. M. Colbert, *Int. J. Mod. Phys.* **D13**, 1 (2004), astro-ph/0308402.
  - [37] K. Makishima et al., *Astrophys. J.* **535**, 632 (2000), astro-ph/0001009.
  - [38] R. R. Islam, J. E. Taylor, and J. Silk, *Mon. Not. Roy. Astron. Soc.* **354**, 427 (2004), astro-ph/0307171.
  - [39] M. C. Begelman, *Astrophys. J.* **568**, L97 (2002), astro-ph/0203030.

- [40] A. R. King, M. B. Davies, M. J. Ward, G. Fabbiano, and M. Elvis, *Astrophys. J.* **552**, L109 (2001), astro-ph/0104333.
- [41] D. A. Swartz, K. K. Ghosh, A. F. Tennant, and K.-W. Wu (2004), astro-ph/0405498.
- [42] X. Fan et al. (SDSS), *Astron. J.* **122**, 2833 (2001), astro-ph/0108063.
- [43] A. J. Barth, P. Martini, C. H. Nelson, and L. C. Ho, *Astrophys. J.* **594**, L95 (2003), astro-ph/0308005.
- [44] C. J. Willott, R. J. McLure, and M. J. Jarvis, *Astrophys. J.* **587**, L15 (2003), astro-ph/0303062.
- [45] Z. Haiman and A. Loeb, *Astrophys. J.* **552**, 647 (2001), astro-ph/0011529.
- [46] S. M. Koushiappas, J. S. Bullock, and A. Dekel, *Mon. Not. Roy. Astron. Soc.* **354**, 292 (2004), astro-ph/0311487.
- [47] S. M. Koushiappas and A. R. Zentner, *Astrophys. J.* **639**, 7 (2006), astro-ph/0503511.
- [48] J. F. Navarro, C. S. Frenk, and S. D. M. White, *Astrophys. J.* **490**, 493 (1997), astro-ph/9611107.
- [49] G. L. Bryan and M. L. Norman, *Astrophys. J.* **495**, 80 (1998), astro-ph/9710107.
- [50] P. Gondolo and J. Silk, *Phys. Rev. Lett.* **83**, 1719 (1999), astro-ph/9906391.
- [51] P. Gondolo et al., *JCAP* **0407**, 008 (2004), astro-ph/0406204.
- [52] T. Sjostrand, *Comput. Phys. Commun.* **82**, 74 (1994).
- [53] T. Sjostrand (1995), hep-ph/9508391.
- [54] N. Fornengo, L. Pieri, and S. Scopel, *Phys. Rev.* **D70**, 103529 (2004), hep-ph/0407342.
- [55] G. Bertone, T. Bringmann, R. Rando, G. Busetto, and A. Morselli (2006), astro-ph/0612387.
- [56] S. Profumo, *Phys. Rev.* **D72**, 103521 (2005), astro-ph/0508628.
- [57] M. Cirelli, M. Kadastik, M. Raidal, and A. Strumia (2008), 0809.2409.
- [58] A. W. Strong, I. V. Moskalenko, and O. Reimer, *Astrophys. J.* **613**, 962 (2004), astro-ph/0406254.
- [59] R. K. Sheth and G. Tormen, *Mon. Not. Roy. Astron. Soc.* **308**, 119 (1999), astro-ph/9901122.
- [60] D. J. Eisenstein and W. Hu, *Astrophys. J.* **511**, 5 (1997), astro-ph/9710252.
- [61] S. Ando, E. Komatsu, T. Narumoto, and T. Totani, *Mon. Not. Roy. Astron. Soc.* **376**, 1635 (2007), astro-ph/0610155.
- [62] H. J. Mo and S. D. M. White, *Mon. Not. Roy. Astron. Soc.* **282**, 347 (1996), astro-ph/9512127.
- [63] S. Profumo, *Phys. Rev.* **D78**, 023507 (2008), 0806.2150.
- [64] <http://coss.c.nasa.gov/docs/cgro/cgro/egret.htm>.
- [65] W. B. Atwood (GLAST), *Nucl. Instrum. Meth.* **A342**, 302 (1994).
- [66] P. F. Michelson (GLAST-LAT), *AIP Conf. Proc.* **921**, 8 (2007).
- [67] <http://www-glast.slac.stanford.edu>.